



Expertise
and insight
for the future

Jussi Airaksinen

Design and Validation of an IGBT Surface Temperature Measurement System

Metropolia University of Applied Sciences

Bachelor of Engineering

Degree Programme in Electronics

Bachelor's Thesis

20.11.2018

Author Title	Jussi Airaksinen Design and Validation of an IGBT Surface Temperature Measurement System
Number of Pages Date	37 pages 20 November 2018
Degree	Bachelor of Engineering
Degree Programme	Degree Programme in Electronics
Professional Major	
Instructors	Veli-Matti Liias, Senior Design Engineer (ABB Oy) Esko Tattari, Senior Lecturer (Metropolia UAS)
<p>The purpose of this work was to design a measurement system to measure IGBT surface temperature when IGBT switches and to be able to compare actual surface temperature to a normal heatsink measurement.</p> <p>In semiconductors, component temperature has a huge effect in reliability and product life time. Actual temperature measurements help in life time expectation estimations.</p> <p>Measurement board was designed and validated to able to measure IGBT surface temperatures while modulating. Validation measurements were performed using IGBT module with pre-installed thermocouple. As IGBT environment has high level of electromagnetic interference, design and validation methods includes filtering possibilities.</p> <p>The resulting design can measure IGBT surface temperature measurements in a few specific cases. The original target of measuring temperature variation when IGBT switches is not possible due to filtering not being able to handle all the switching noise. However, junction temperature can be compared to heatsink temperature.</p>	
Keywords	IGBT, Junction, Temperature, Thermocouple, VFD, Inverter

<p>Tekijä Otsikko</p> <p>Sivumäärä Päivämäärä</p>	<p>Jussi Airaksinen IGBT pintalämpötilamittausjärjestelmän suunnittelu ja validointi</p> <p>37 sivua 20.11.2018</p>
<p>Tutkinto</p>	<p>Insinööri (AMK)</p>
<p>Koulutusohjelma</p>	<p>Elektroniikka</p>
<p>Suuntautumisvaihtoehto</p>	
<p>Ohjaajat</p>	<p>Suunnittelija Veli-Matti Liias Lehtori Esko Tattari</p>
<p>Työn tarkoituksena oli toteuttaa mittausjärjestelmä, jolla pystytään mittaamaan IGBT:n pintalämpötilaa IGBT:tä kytkettäessä, sekä saada vertailukelpoisia tuloksia aikaisemmin jäähdytyslevystä mitattuihin lämpötiloihin verrattuna.</p> <p>Puolijohdekomponenttien lämpötila vaikuttaa merkittävästi niiden luotettavuuteen sekä elinajanodotteeseen. Konkreettiset lämpötilamittaukset tukevat aikaisempia elinikälaskelmia.</p> <p>Työssä suunniteltiin, toteutettiin ja validoitiin mittausjärjestelmä, jolla pystytään mittaamaan valmistajan IGBT moduulin sisälle asentamaa termoparia. Mittausympäristön tiedettiin olevan erityisen häiriöaltis, joten suunnittelu- ja validointimetodit sisälsivät mahdollisimman paljon erilaisia suodatusmahdollisuuksia.</p> <p>Toteutetulla mittausjärjestelmällä pystytään mittaamaan IGBT:n pintalämpötilaa muutamissa erityistilanteissa. Alkuperäinen tavoite, IGBT:n kytkennän aiheuttaman lämpötilan nousun mittaaminen jäi tavoittamatta, sillä kytkentähäiriöiden suodattaminen osoittautui mahdottomaksi. Sen sijaan pintalämpötilaa pystytään vertaamaan aikaisempiin jäähdytyslevystä mitattuihin lämpötiloihin.</p>	
<p>Avainsanat</p>	<p>IGBT, lämpötila, termopari, taajuusmuuttaja, invertteri</p>

Contents

List of Figures

List of Tables

List of Abbreviations

1	Introduction	1
2	Background	2
2.1	Variable Frequency Drive	2
2.2	Insulated-gate Bipolar Transistor	4
2.3	Thermocouples	6
2.3.1	Reference Junction Compensation	9
2.4	Isolation Techniques	10
2.5	Delta-Sigma ADC	11
3	Main Components	12
3.1	ACS580	12
3.2	MiniSKiiP	13
3.3	PicoScope	14
4	Design	15
4.1	Safety Considerations	15
4.2	Different Design Concepts	16
4.3	Simulation	16
4.4	Components	19
4.4.1	Thermocouple Amplifier	19
4.4.2	Isolation Amplifier	19
4.4.3	Power Supply	20
4.5	Schematic	20
4.6	Layout	22
4.7	Enclosure	24
5	Verification	25
5.1	Nonlinearity Error Correction	25
5.2	Board Verification	26
5.3	Initial Results	28
5.4	Modifications	29
5.5	End Results	30
5.6	Future Considerations, Improvements and Measurements	32
6	Conclusions	34
	References	35

List of Figures

- Figure 1 – Typical high-level schematic of an VFD
- Figure 2 – Simplified output voltage and current when using PWM control
- Figure 3 – IGBT cross section and equivalent circuit
- Figure 4 – Main sources of IGBT losses
- Figure 5 – Diagram of thermocouple measurement
- Figure 6 – Seebeck effect voltage vs. temperature with different types of thermocouples
- Figure 7 – Ice bath reference junction compensation
- Figure 8 – Block diagram of first order $\Delta\Sigma$ modulator
- Figure 9 – ABB ACS580 R2 unit
- Figure 10 – Semikron 24NAB12T4V1 MiniSKiiP
- Figure 11 – PicoScope 3406D MSO
- Figure 12 – Simulation schematics on both concepts
- Figure 13 – Simulation waveforms of both concepts
- Figure 14 – Block diagram of the AD849x IC
- Figure 15 – Functional diagram of the AMC1311 Isolation Amplifier
- Figure 16 – Block diagram of the measurement system
- Figure 17 – Schematic of the non-isolated parts of the measurement system
- Figure 18 – Schematic of the isolated parts of the measurement system
- Figure 19 – Top side of the layout design
- Figure 20 – Bottom side of the layout design
- Figure 21 – Enclosure design
- Figure 22 – Temperature change response check
- Figure 23 – Measurement system accuracy testing
- Figure 24 – Comparison of non-isolated and isolated outputs
- Figure 25 – First measurements
- Figure 26 – X-ray images of Semikron provided MiniSKiiP
- Figure 27 – Comparison between junction and heatsink temperature
- Figure 28 – Lower side IGBT temperature change in one cycle

List of Tables

Table 1 – Comparison chart of the most typical thermocouple types

Table 2 – Relevant part of the nonlinearity error correction table reprinted from AN-1087

List of Abbreviations

AC	Alternating Current
VFD	Variable Frequency Drive
DC	Direct Current
IGBT	Insulated-Gate Bipolar Transistor
PWM	Pulse Width Modulation
MOSFET	Metal-Oxide-Semiconductor Field-Effect Transistor
BJT	Bipolar Junction Transistor
EMI	Electromagnetic Interference
IC	Integrated Circuit
PCB	Printed Circuit Board
LED	Light-Emitting Diode
OOK	On-Off Keying
$\Delta\Sigma$	Delta-Sigma
ADC	Analog-to-Digital Conversion
SAR	Successive Approximation Register
HPTP	High Performance Thermal Paste
MSO	Mixed Signal Oscilloscopes
ESD	Electrostatic Discharge
DSP	Digital Signal Processing
NTC	Negative Temperature Coefficient

1 Introduction

The last few decades have seen great development in industry relevant electrical equipment. Variable Frequency Drives have become the most popular way of controlling motors in industrial applications. Manufacturing good and reliable VFDs has become more and more important, as equipment failures or end of life changes in the end user applications can lead to lengthy downtimes.

While there are multiple different failure modes that are not related to maximum operating temperature, semiconductor temperatures play a vital role in reliability and lifetime of a product. Even slightly lowering the operational temperature of a component inside a product can lead to much longer life time expectation. As a rule of thumb, it is usually told that every 10°C increase in component temperature leads life time expectation to be cut in half.

Lifetime expectations can be normally calculated using specific models that takes into consideration different kind of use case parameters, such as ambient temperature, other environment factors and load requirements.

The goal of this study is to design a way to measure IGBT surface temperatures. Having actual measurement data is crucial, as it can used to support lifetime expectation calculations. For the end user, this means more reliable VFDs, as the calculation models can be tweaked to consider actual measured temperatures.

2 Background

2.1 Variable Frequency Drive

Variable frequency drive is an electromechanical device, which is commonly used to drive AC motors. VFD allows for frequency and torque control of an electric motor and provides feedback of the system for monitoring use. As a control method, VFDs has become popular as they are relatively cheap, accurate, easy to use and energy efficient systems compared to previous methods of controlling motors.

As electric motors in industrial applications consume about 70% of the industrial electrical energy, VFDs has become the way to lower consumed energy. Typical VFD efficiency is around 95-99%. [1]

VFDs can be split into two different categories, indirect and direct drives. Difference between these are conversion method, direct drives do not have any intermediate DC link, thus making an AC-AC conversion to the motor. Indirect drives first rectify AC to DC, then DC is inverted back to AC. Indirect drives are more commonly used when output power requirements are relatively small, starting from few hundred watts, while direct drives are used when high power rating, starting from few megawatts, is required. Direct drives are being gradually replaced as faster switching based solutions have become more common [2].

Most of the current applications use indirect frequency drives as in most use cases power rating of few kilowatts is needed. Commonly indirect VFDs use 3-phase diode bridge to rectify supplied AC voltage to DC, capacitors in DC bus to filter ripple and store energy and IGBT based inverter to switch DC back to AC current that is supplied to motor.

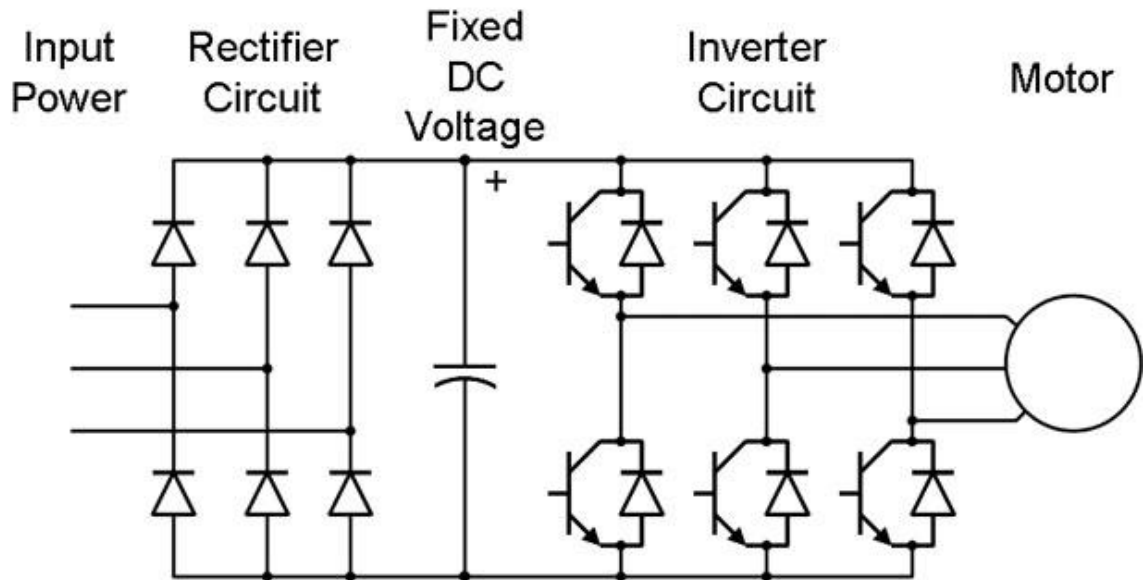


Figure 1: Typical high-level schematic of an VFD [3]

Figure 1 shows a working diagram of a typical frequency drive. This type of VFD is not capable of regenerative braking back to supply network, all excess DC link voltage is supplied to brake resistor via brake chopper IGBT and turned into heat. Otherwise regenerative drives work on a similar principle, only passive rectifier circuit is changed to active IGBT inverter circuit which is capable of supplying electricity back to supply network.

Inverter circuit uses PWM controlled IGBTs to supply motor. As a high side IGBT is in conductive state, DC bus is directly connected into motor. Current flows through the motor when also one of the low side IGBTs is closed. All 3-phases go through similar on-off pattern, called switching, to create necessary supply voltage for the rotor to spin.

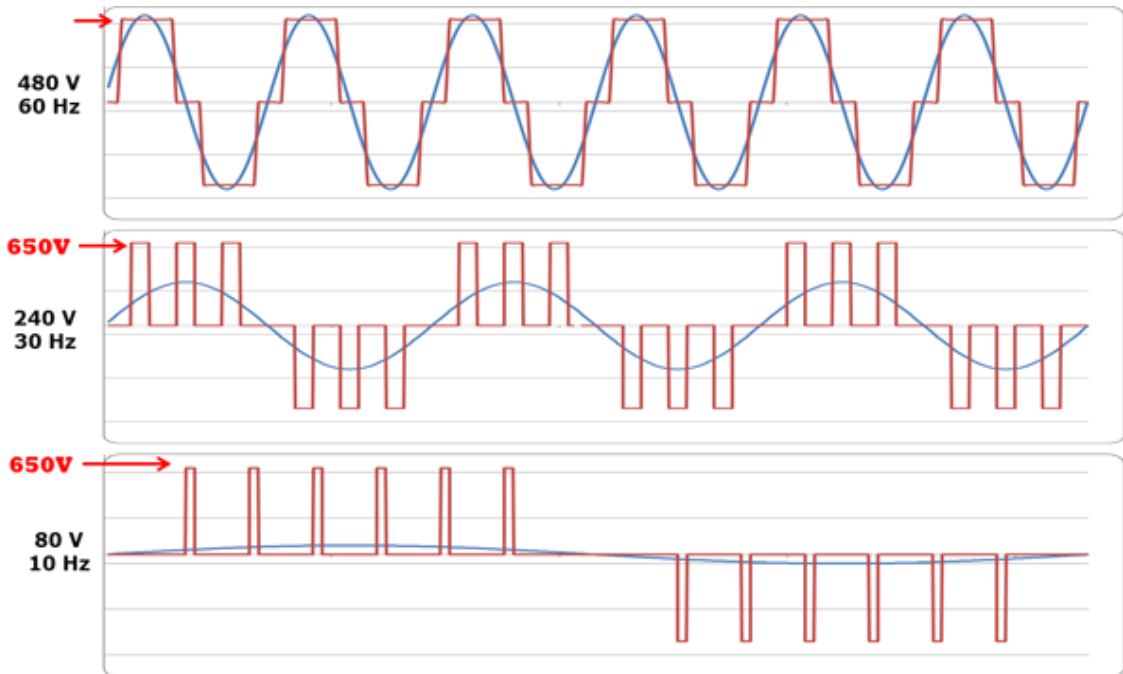


Figure 2: Simplified output voltage and current when using PWM control and 480V supply voltage [4]

As a motor is an inductive load and cannot react fast enough to voltage switching, current seen by motor is smoothed to close of a sine wave as shown by Figure 2. This allows for the motor spin smoothly at the controlled frequency and if switching pattern duty cycle and frequency were to be reduced, current at the motor would change more slowly resulting in lower motor speed.

2.2 Insulated-gate Bipolar Transistor

Insulated-gate bipolar transistor (IGBT) is the most commonly used switching device in VFDs. IGBT combines the best parts of MOSFET and BJT by having high input impedance and simple gate drive characteristics similar to MOSFETs and low on-state power loss, thus being able to handle both high currents and voltages. [5]

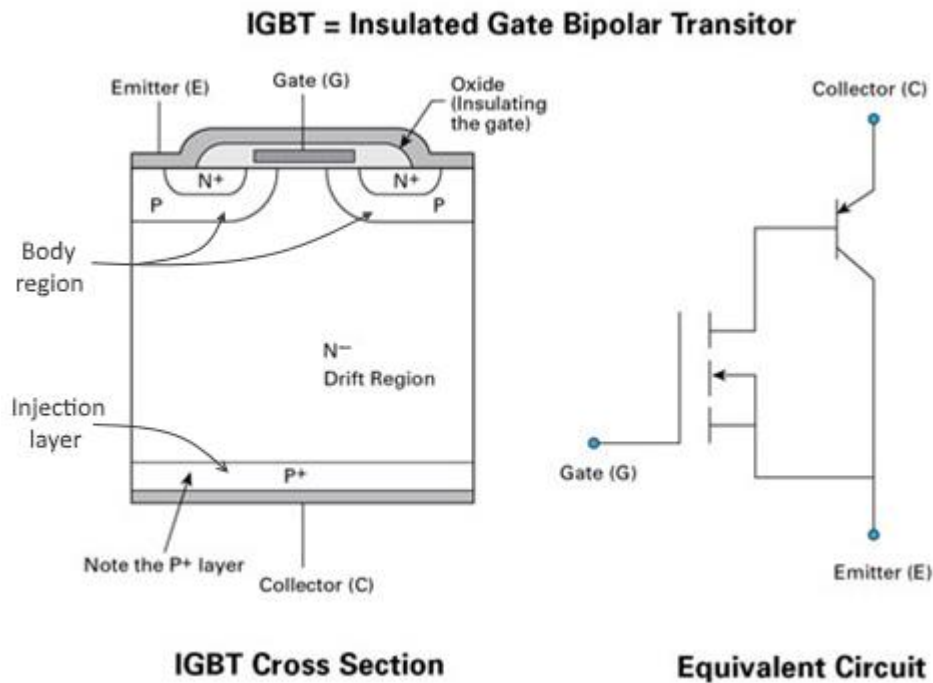


Figure 3: IGBT cross section and equivalent circuit [6]

As Figure 3 shows, IGBT has four alternating P-N junctions. IGBT effectively works very similarly compared to a power MOSFET. When positive collector-emitter voltage is applied, IGBT is in forward bias state. This means that electrons from body region and holes from injection layer flood to drift region, making junction between drift region and injection layer conductive. If no gate voltage is applied, no conductive channel is formed through body region. When positive gate voltage is applied, electrons in body region are drawn towards gate terminal. When high enough voltage is applied, known as threshold voltage, enough electrons in body region are drawn and a conductive path for current to flow through body region is formed. [7]

IGBT can often be told to be a variable resistor. When no gate voltage is present, resistance between collector and emitter is very high, but when gate voltage higher than threshold voltage is applied, collector-emitter resistance drops drastically.

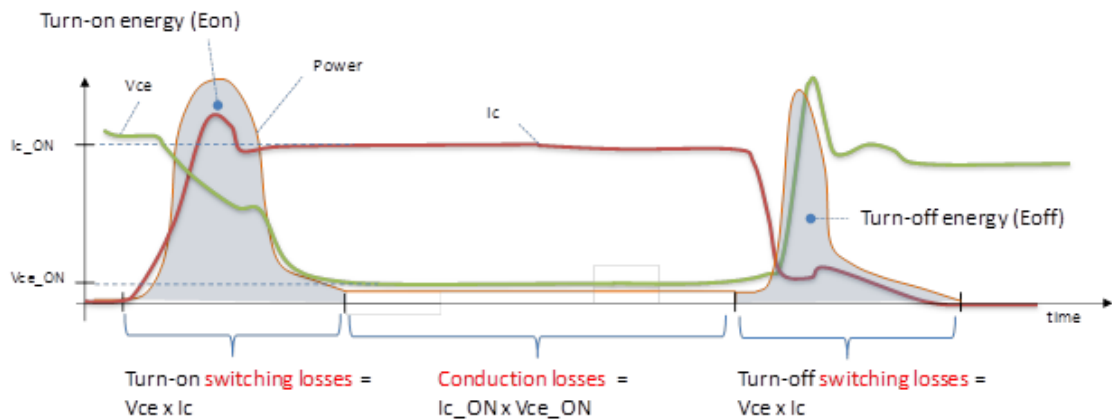


Figure 4: Main sources of IGBT losses [8]

IGBT power losses are coming from switching and conduction losses, shown by figure 4. This energy is turned into heat and dissipated using heatsink connected to IGBT module heat spreading plate.

Turn-on losses happens when IGBT is turned from off state to conductive state. When IGBT gate voltage is applied, collector-emitter voltage starts to drop and collector current rises. This turn-on transient has brief, but large power consumption as voltage and current at the IGBT can simultaneously be quite large. Turn-off losses are reciprocal to turn-on losses and these as combined are known as switching losses.

After the IGBT is turned on, it conducts load dependent current through itself. This current also results in small collector-emitter voltage across the IGBT. This power is called conduction losses.

2.3 Thermocouples

Thermocouple is widely used electric temperature measurement device especially in industries. It is inexpensive to use, small, physically very robust and wide range of temperatures can be measured. Main limitations when using thermocouples are accuracy and small signal voltage, which ranges from microvolts to a few millivolts thus measurement is easily affected by EMI. Thermocouple accuracy typically is a few degrees Celsius, less than that is hard to achieve [9].

Thermocouple consists of two metallic wires and uses thermoelectric effect to measure temperature. Metallic wires are joined at the end of the thermocouple, this join is called measurement junction or hot junction. Due to Seebeck effect, thermocouple acts as temperature-voltage transducer and produces temperature-dependent voltage which can be measured across the two metallic wires. The point where thermocouple is connected to measurement system is called reference junction. Typical diagram of thermocouple measurement can be seen in Figure 5.

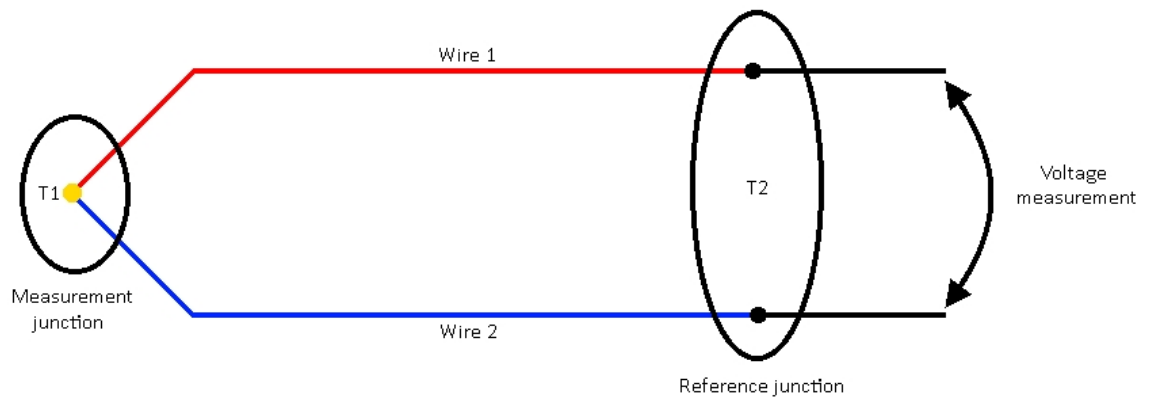


Figure 5: Diagram of thermocouple measurement

Measured voltage across reference junction turns out to be:

$$E(T) = \int_{T_2}^{T_1} S_{Wire\ 1\ Wire\ 2} dT = \int_{T_2}^{T_1} (S_{Wire\ 1}(T) - S_{Wire\ 2}(T)) dT \quad (1)$$

Where:

- $S_{Wire\ 1\ Wire\ 2}$ = Seebeck coefficient of the thermocouple
- T1 = Temperature at measurement junction
- T2 = Temperature at reference junction
- $S_{Wire\ 1}$ = Seebeck coefficient of positive measurement wire
- $S_{Wire\ 2}$ = Seebeck coefficient of negative measurement wire

A few things can be understood from the Seebeck effect formula. Different metallic materials are required to be used as conductors in thermocouple. If the same material is used in both of the thermocouple wires, no voltage is generated at the measurement junction and no temperature-dependent voltage can be measured. Also, there must be a temperature difference between measurement junction and reference junction. [10]

Table 1: Comparison chart of the most used thermocouple types [11]

Thermocouple Types			
Type	Composition	Sensitivity	Temperature range
Type B	(+) Platinum - 30% Rhodium (-) Platinum - 6% Rhodium	5 to 10 $\mu\text{V}/^\circ\text{C}$	+250 to +1820 $^\circ\text{C}$
Type E	(+) Chromel (Ni-Cr) (-) Constantan (Cu-Ni)	40 to 80 $\mu\text{V}/^\circ\text{C}$	-270 to +1000 $^\circ\text{C}$
Type J	(+) Iron (-) Constantan (Cu-Ni)	50 to 60 $\mu\text{V}/^\circ\text{C}$	-210 to +1200 $^\circ\text{C}$
Type K	(+) Chromel (Ni-Cr) (-) Alumel (Ni-Al)	28 to 42 $\mu\text{V}/^\circ\text{C}$	-250 to +1250 $^\circ\text{C}$
Type N	(+) Nicrosil (Ni-Cr-Si) (-) Nisil (Ni-Si-Mg)	24 to 38 $\mu\text{V}/^\circ\text{C}$	-250 to +1300 $^\circ\text{C}$
Type R	(+) Platinum (-) Platinum - 13% Rhodium	8 to 14 $\mu\text{V}/^\circ\text{C}$	-50 to +1768 $^\circ\text{C}$
Type S	(+) Platinum (-) Platinum - 10% Rhodium	8 to 12 $\mu\text{V}/^\circ\text{C}$	-50 to +1768 $^\circ\text{C}$
Type T	(+) Copper (-) Constantan (Cu-Ni)	17 to 58 $\mu\text{V}/^\circ\text{C}$	-250 to +400 $^\circ\text{C}$

Multiple different thermocouples, which are denoted as letters, can be made by combining different metals in thermocouple leads. Table 1 shows some of the most commonly used thermocouple types, their Seebeck coefficients and temperature ranges. This makes thermocouples suitable for multiple different measurement cases, as required characteristics can be achieved by combining different metals.

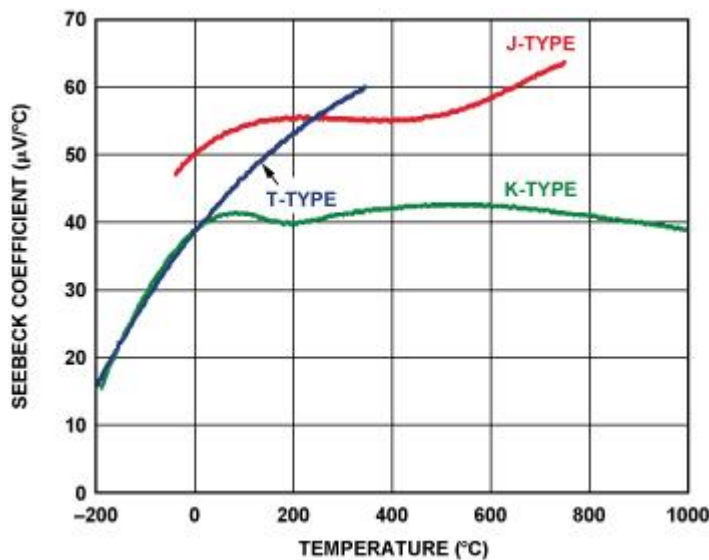


Figure 6: Seebeck effect voltage vs. temperature graph with different types of thermocouples [12]

The most commonly used thermocouple types are J and K due to their relatively linear characteristics. As can be seen from figure 6, K-type thermocouple has quite linear sensitivity for almost its whole measurement range, being at around $41\mu\text{V}/^\circ\text{C}$ except for under 0°C . Using J-type thermocouple, while not being as linear compared to K-type, can

be also beneficial because better sensitivity makes voltage processing easier later in the measurement system. Compared to T-type thermocouple, J- and K-type thermocouples offer much easier measurement systems to be built as linearity does not change as drastically between different temperatures and use of a nonlinearity error correction table is not required in all cases.

2.3.1 Reference Junction Compensation

As previously stated, reference junction temperature affects thermocouple measurements and for a thermocouple measurement to work properly, reference junction compensation must be done. Reference junction compensation is also known as cold junction compensation.

Thermocouple lead has to be connected to measurement system for example via terminal or direct soldering. This results in similar voltage to be generated as in measurement junction, thus creating error in the measurement. This error is the same as temperature in reference junction.

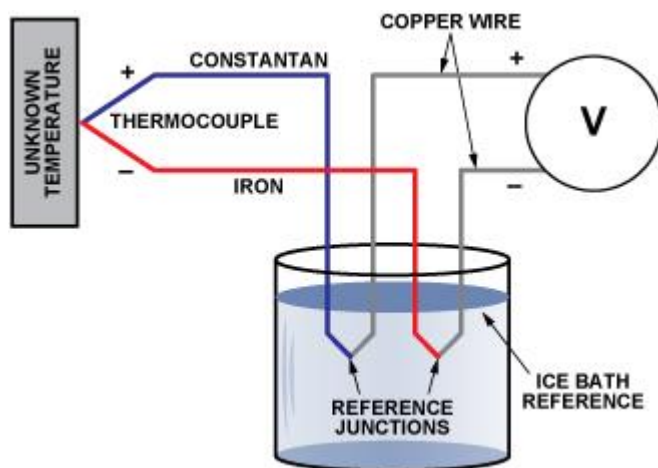


Figure 7: Ice bath reference junction compensation [12]

In early days, reference junction compensation was done placing reference junction into ice bath and effectively fixing reference junction to as close as possible to 0°C. This method is shown in figure 7 and results in no voltage to be generated at the reference junction. While this is still completely valid method to use, it is not very practical and in most cases completely impossible.

More common option for compensation is to measure temperature at the reference junction. If reference junction temperature is known, a lookup table can be used to determine its effect on the measurement and that effect can be added back to measurement signal before amplification. Most of the thermocouple measurement ICs have internal temperature sensor and reference junction compensation. Usually thermocouple measurement IC is located near reference junction on PCB, so this temperature sensor can be used for compensation. While there might be slight error due to placement of the temperature sensor, this error is negligible in most cases.

2.4 Isolation Techniques

Electrically separating two different parts of the same circuit is called isolation. Most likely, isolation is used in applications that require communication between two circuits that have different ground level. This also offers safety benefits, as dangerous high voltage circuits can be isolated from user level potential. Other possible use case is improving measurement accuracy by breaking ground loops

Mainly, there are three different isolation techniques, capacitive, inductive and optical. While all of these achieve similar results, they all work differently.

Optical isolation transmits data across isolation barrier using an LED and photodiode, thus light is used for transmitting through a transparent insulator. While being mostly immune to electric and magnetic fields, opto-isolators have lower data rate compared to other techniques due to being limited by LED switching speed. Design also has to take into account aging of the LED and yellowing of the insulator material, both reducing the performance of an opto-isolator [13].

Inductive isolation uses inductive coupling through a transformer to isolate signal across isolation barrier. It has higher data rates than opto-isolators but is susceptible to outside magnetic fields. Typical inductive isolation solutions are also larger in size than other isolators. [13]

Capacitive isolation uses electric field for signal transferring. OOK modulation is used to turn high input signal into high frequency carrier signal through isolation barrier, while capacitor blocks DC voltage. After isolation barrier, demodulator is used to reconstruct

previous input signal. Analog input signals can also be used by utilizing for example $\Delta\Sigma$ ADC before OOK modulation. Capacitive isolators have the highest data-rate out of the three isolation techniques [13].

2.5 Delta-Sigma ADC

Delta-Sigma ($\Delta\Sigma$) ADC is one of the most popular ADC types currently. Compared to other popular ADC, SAR, it offers higher resolution at the cost of sampling rate [14]. High resolution makes $\Delta\Sigma$ ADC great for applications where high precision is required, like thermocouple measurements.

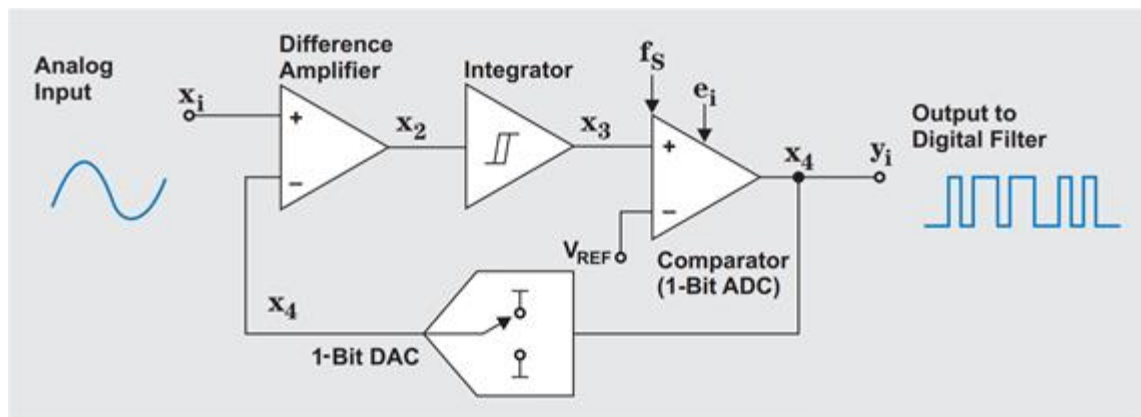


Figure 8: Block diagram of a first order $\Delta\Sigma$ modulator [15]

Figure 8 shows block diagram of an $\Delta\Sigma$ ADC. It uses oversampling to convert analog signal at the input to single bit modulated pulse wave. Delta-Sigma modulator works with a feedback loop, as it always differentiates output bit with input signal. This voltage is then supplied into an integrator, where integrator output progresses in a positive or negative direction. Depending on the previous state, 1-bit comparator then flips the output bit if comparator input voltage polarity is switched. Depending on output bit state, 1-bit DAC is connected to either positive or negative reference voltage and supplied back into a difference amplifier. [15]

$\Delta\Sigma$ ADC output state can be calculated: [15]

$$y_i = x_{i-1} + (e_i - e_{i-1}) \quad (2)$$

Where:

- X_4 = Output signal of the $\Delta\Sigma$ ADC
- X_i, X_{i-1} = Current and previous input signals
- e_i = Current quantization error
- e_{i-1} = Previous quantization error

Output signal of the Delta-Sigma modulation becomes modulated pulse wave which is proportional to input signal. Output signal can be easily filtered back into input signal by averaging the modulator output waveform.

3 Main Components

3.1 ACS580

In this measurement setup ABB ACS580 series VFDs was used. These are common, general purpose drives, which handle most kind of different use cases. ACS580 series has frame sizes ranging from R0 to R11 which gives good variety of choices between 0.75kW and 250kW units [16].



Figure 9: ABB ACS580 R2 unit [16]

ACS580 drive uses a pinstrip connection for communication between main board and control board. This pinstrip contains digital and analog signals such as fault communication and IGBT gate driver signals. All pinstrip signals can be read using specifically designed logging board and displayed simultaneously on oscilloscope screen. This logging board is used later in the measurements to compare IGBT control signals to temperature reading.

3.2 MiniSKiiP

ACS580 series uses Semikron manufactured MiniSKiiP modules. MiniSKiiP modules include 3-phase rectifier and inverter circuits and a brake chopper IGBT in small package. Assembly of a MiniSKiiP module is simple because it uses spring contacts for electrical connection to a PCB. Compared to conventional modules, no soldering or special tools are required on installation process [17].

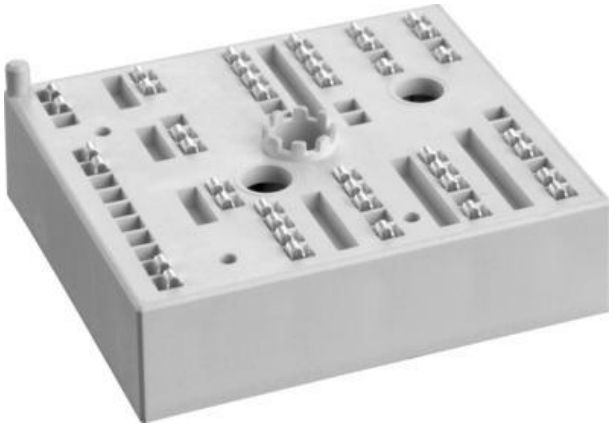


Figure 10: Semikron 24NAB12T4V1 MiniSKiiP [18]

Figure 10 shows the MiniSKiiP used in 11kW R2 ACS580 drives. This specific module allows for a maximum continuous collector current of 35A, but similar kind of modules can be had up until 400A [17].

Semikron provided us MiniSKiiPs with pre-installed J-type thermocouples for R1, R2 and R3 ACS580 drives. Thermocouple is installed on lower side, V-phase IGBT on all modules. These modules also came with pre-installed HPTP, reducing thermal resistance between heat spreader and heatsink, thus lowering IGBT junction temperatures.

3.3 PicoScope

PicoScope 3406D MSO is used in the measurements. It offers 200 MHz analog bandwidth, 1G/s real-time sampling, 4 analog channels and 16 channel logic analyzer. [19]



Figure 11: PicoScope 3406D MSO [19]

PicoScope is a handy device for ACS580 measurements, as pinstrip can be easily and safely measured using its digital channels. PicoScope uses computer software as a front end. One of the main benefits of using these kinds of oscilloscopes are measurement length and post processing features. PicoScope can also be powered via external power bank, thus removing the need to use an isolation transformer. As pinstrip measurements are referenced to UDC-, powering the PicoScope without isolation transformer from a wall outlet would result into current leaking to test area safety ground.

4 Design

4.1 Safety Considerations

Safety of the measurement system must be considered as measurement thermocouple is directly connected on top of the IGBT. This causes the thermocouple leads to be in the same voltage potential as the IGBT itself, so un-isolated parts of the circuit can give high voltage electric shocks if touched.

While the PCB can be isolated and placed out of fingers reach, measurement devices also must be considered. As PicoScope measurement setup takes direct digital measurements from ACS580 unit pinstrip, all the measurements are referenced to UDC- potential. This causes the whole measurement system to be referenced to high voltage potential and to be dangerous for the person making these measurements.

Currently thermocouple is connected to lower side of the inverter, but for future use the measurement setup also has to be able to handle thermocouple to be connected on the high side IGBTs. Due to this, PCB must be designed to have isolation from high voltage parts to protect tester, measurement devices and the ACS580 unit itself. When thermocouple is connected to lower side IGBTs, isolation amplifier is not necessary to use as PicoScope potential is already at UDC- due to pinstrip measurements, so design also needs to include a way to take measurements without using isolation. When high side IGBTs are to be measured, temperature measurement has to be isolated from the rest of the measurement system, as connecting it without isolation would results in direct frequency drive DC link short circuit through PicoScope and potentially damaging every part of the measurement system.

4.2 Different Design Concepts

At the start of the project, two different design concepts were simulated. Main difference between these was circuit complexity and compatibility with different types of thermocouples.

First design included LT1025 reference junction compensator IC which output was amplified with LTC1049 operational amplifier to get reasonable output scaling. Main benefit of this system was that it is compatible with multiple different thermocouples, such as J, K, R and T. As it also has external output amplifier, scaling of the output voltage can be changed as needed.

Second concept consists of AD8496 thermocouple amplifier IC which integrates reference junction compensation and output amplifier into same package. This makes circuit design much easier and simpler, requiring far less components compared to the first design. Downside in this system is that its only compatible with one type of thermocouple, depending on the IC used as the amplifier gain is fixed. Analog Devices provide different kind of thermocouple amplifiers, which are compatible either with J or K-type thermocouples.

4.3 Simulation

Simulation of the design is always important, as it can show design errors or ways to improve the design early in the design phase. It can be also used to easily test how design responds to different components; in this case hardware filtering solutions can be tested even before board itself is designed.

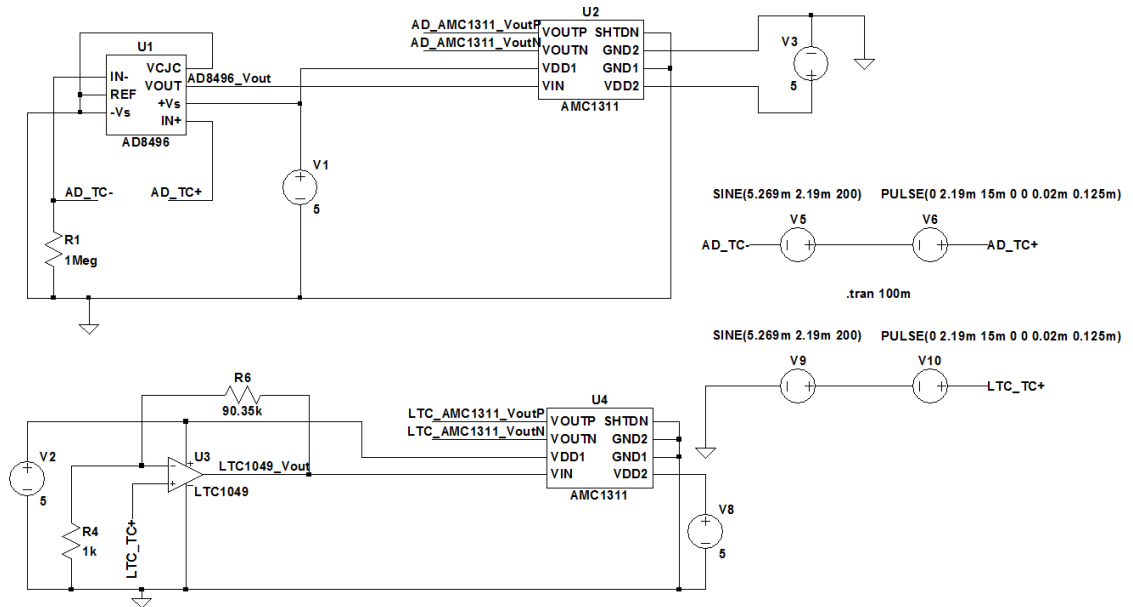


Figure 12: Simulation schematics on both concepts

Both designs were simulated on one schematic using LTSpice simulation software, which is shown in figure 12. Spice models for all components can be download on their manufacturer's website.

AD8496 design is also easier to design, as it does not need external amplification and resistor tolerances in amplification circuit are not going to be an issue. One benefit of the external amplifier is that amplification can be set higher or lower depending on the use case.

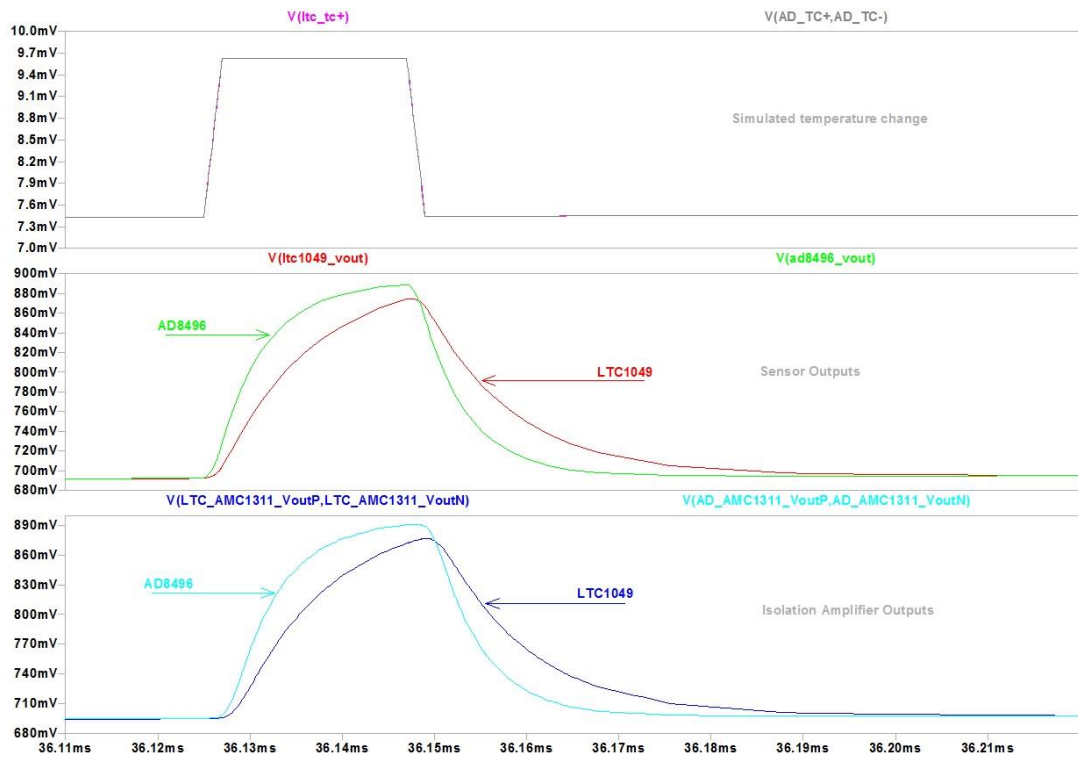


Figure 13: Simulated waveforms on both concepts

Simulated temperature change is $+20^{\circ}\text{C}$ at 4kHz, simulating switching losses on top of base 50Hz sine wave changing $\pm 40^{\circ}\text{C}$ at every cycle. While temperature change being more than predicted, it gives more information about performance differences between the concepts.

As can be seen from figure 13, AD8496 based concept is slightly faster than LTC1049 based concept, even when reference junction compensation was removed from the circuit. Based on simulations, AD8496 is chosen to be used as being a faster system combined with the ease of use in AD8496 IC makes it a better choice. Also, it seems that the use of an AMC1311 isolation amplifier does not add any delay to the measurement.

4.4 Components

4.4.1 Thermocouple Amplifier

Thermocouple amplifier selected for this measurement system is AD8496 IC from Analog Devices. AD8496 is pretrimmed for J-type thermocouple and integrates instrumental amplifier with reference junction compensation. Output voltage is amplified to $5\text{mV}/^\circ\text{C}$. [20]

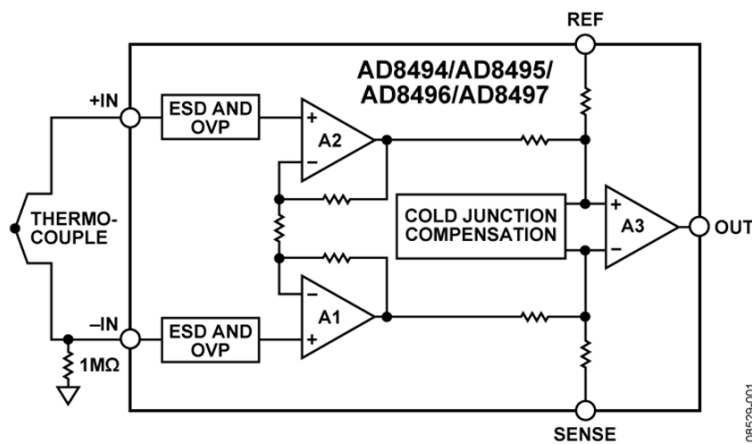


Figure 14: Block diagram of the AD849x IC [20]

As can be seen from figure 14, AD849x ICs also feature ESD and overvoltage protections. Reference pin can be used to measure temperatures below 0°C even with single sided supply, as it allows for output offset. [20]

4.4.2 Isolation Amplifier

Most of the isolation amplifiers are designed to work with much lower input voltages, such as $\pm 250\text{mV}$, than required in this project. AMC1311 IC offers $0\text{--}2\text{V}$ input range, which is a better option to use than scaling thermocouple amplifier output to match input range of an isolation amplifier which has lower input voltage range. [21]

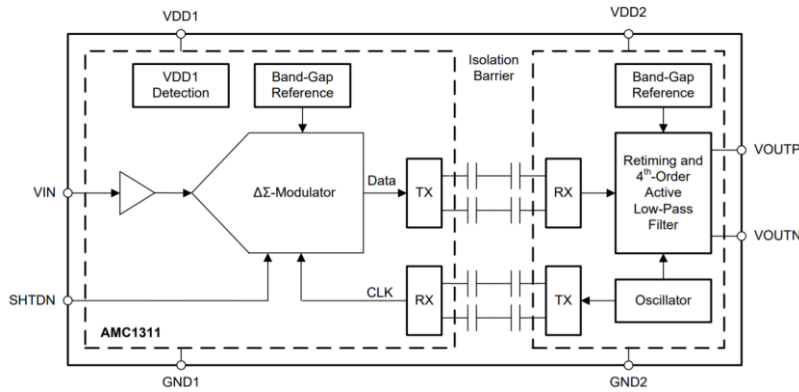


Figure 15: Functional diagram of the AMC1311 Isolation Amplifier [21]

Figure 15 shows the functional block diagram of the AMC1311 IC. As can be seen, AMC1311 uses capacitive isolation and Delta-Sigma modulation to pass signal analog input signal through isolation barrier. Commonly isolation amplifiers are used to isolate shunt resistor voltage, but it can also be used with any voltage sources with high output impedance such as thermocouple amplifiers.

4.4.3 Power Supply

While AD8496 chip allows to use wide range of supply voltages, isolation amplifier requires supply voltage ranging from 3.3V to 5V. It is possible to get this required supply voltage from the VFD, but it would limit the measurement possibilities as ground level would be connected into the frequency drive. The easiest way around this is to use independent supply on the measuring board. This makes it more plug-and-play type of system, where VFD itself does not have to be modified. Also, the isolated side of the measurement board requires its own supply anyway.

Board uses two 9V PP3 batteries, one on each side. This 9V supply is then regulated to a fixed and stable 5V using μ A78M05 voltage regulator which both isolation amplifier and thermocouple amplifier can use as a supply voltage.

4.5 Schematic

Schematic design of the system was quite straightforward and done by PADS. Some of the used components were already available in ABB PADS library, but AD8496 and AMC1311 ICs were missing and had to be done before designing could start. Design

includes optional hardware-based RC filters. These filter components can be installed, if needed, on the thermocouple input, non-isolated output and isolated output.

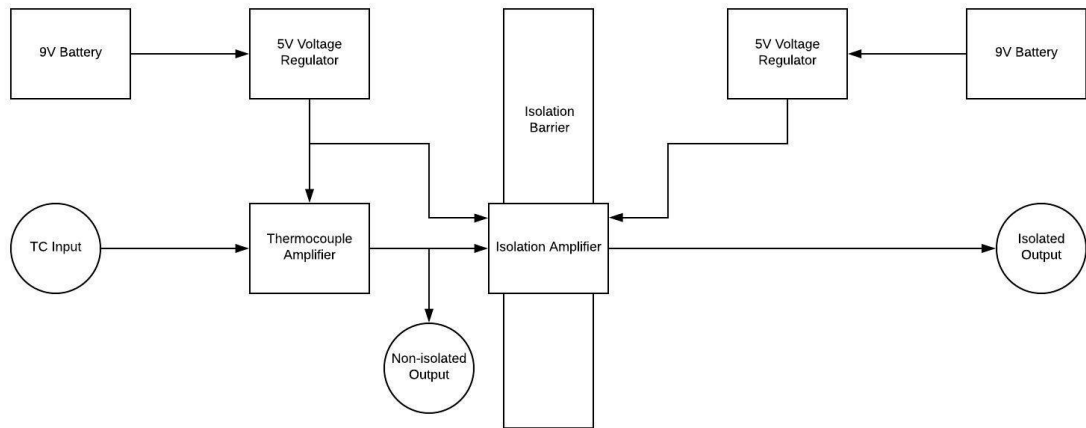


Figure 16: Block diagram of the measurement system

Figure 16 shows the block diagram of the designed measurement system. As can be seen from the block diagram, design was made to as simple as possible without using any of the advanced features included in AD8496 thermocouple amplifier, such as offset adjustment.

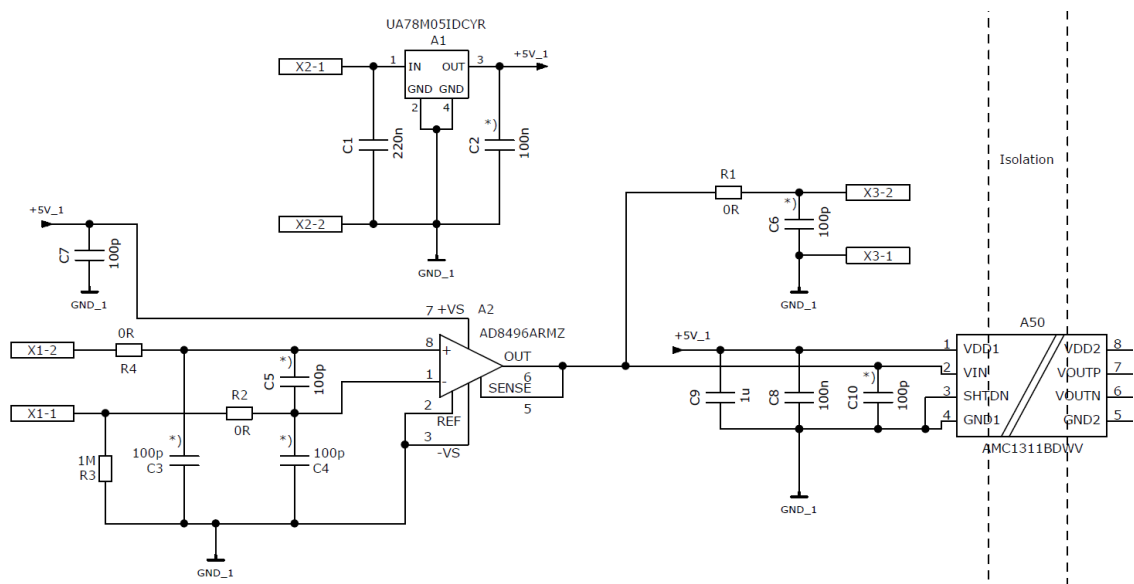


Figure 17: Schematic of the non-isolated parts of the measurement system

Figure 17 shows non-isolated side of the measurement board. It is done mostly by utilizing implementation guides found on every component's datasheet with optional input

and output RC low-pass filtering. Board also features terminal block before isolation amplifier for temperature measurements without isolation.

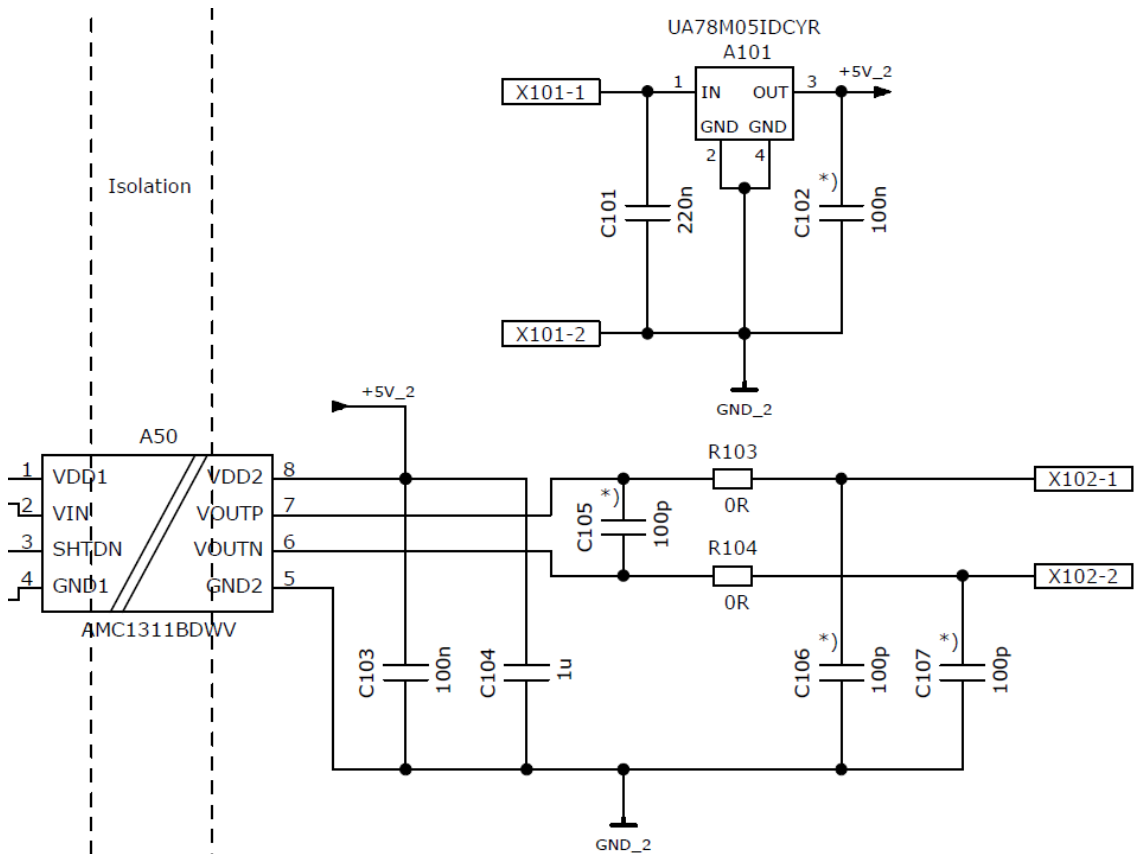


Figure 18: Schematic of the isolated parts of the measurement system

Isolated part of the measurement board includes power supply for the isolation amplifier and optional common and differential mode filtering as can be seen in figure 18. These filters can be bypassed by connecting 0R resistors from AMC1311 output to terminal blocks.

4.6 Layout

Correct layout design needs to consider multiple different things. IC power supply filtering capacitors need to be as close as possible to IC supply pin. Design needs to minimize noise coupling, thus all input and output traces run as closely to each other as possible.

As the components are assembled by hand, all the pads were made slightly larger than normally to ease the assembly. Screw holes with keepout were added to all corners allowing the board to be installed in an enclosure.

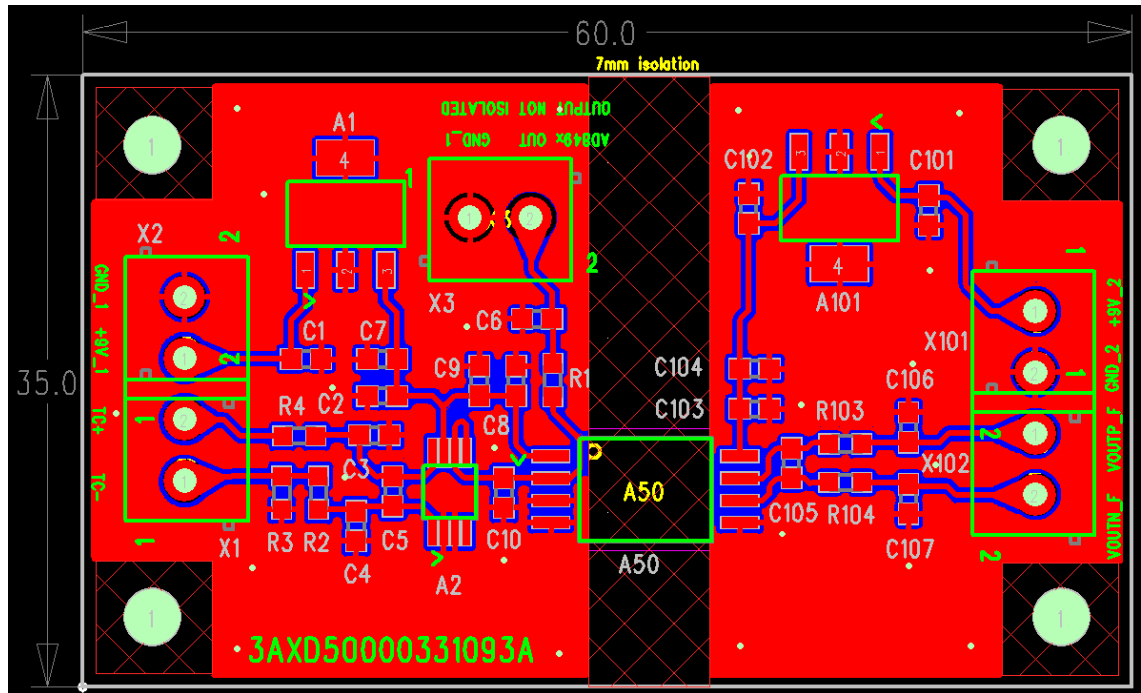


Figure 19: Top side of the layout design

Figure 19 shows top side of the board, which contains all the required components. All terminal block functions are marked using text in silkscreen. Also, all unused space in top side is flooded with ground connection.

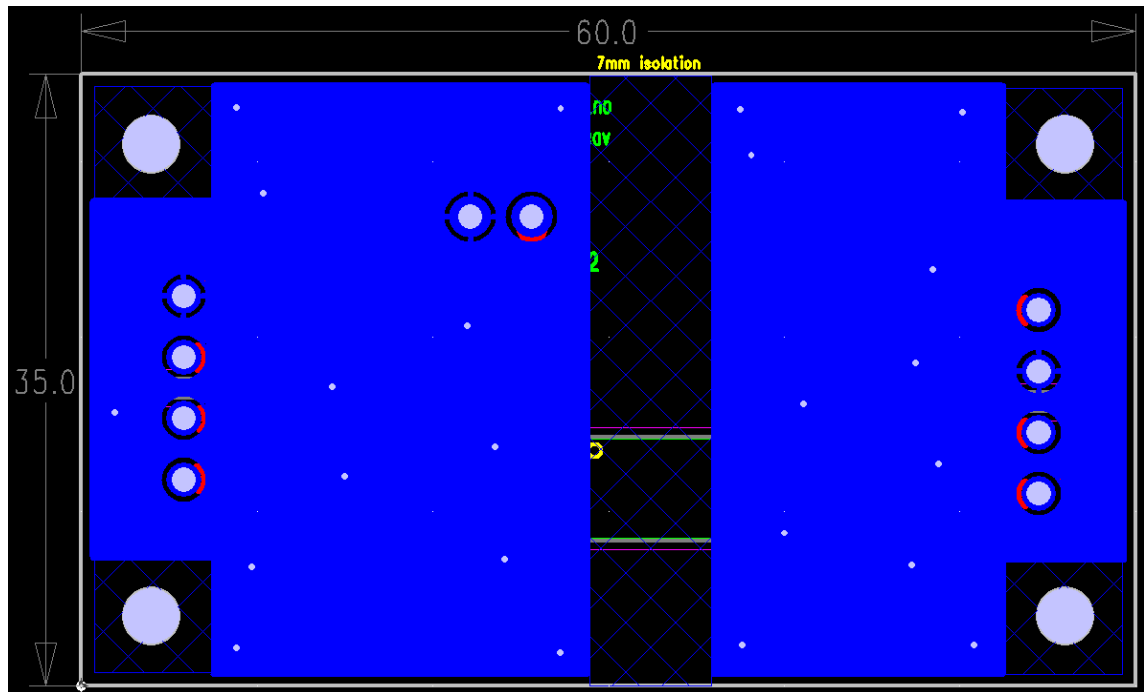


Figure 20: Bottom side of the layout design

As all the components are on the top side, bottom side can be used only for ground layer, making possible ground loops shorter, thus reducing noise. Ground loops are also reduced by using a lot of vias on the board, shown by figure 20.

4.7 Enclosure

As a safety measure against accidental touching of the board, enclosure was designed around the board and printed using a 3D printer. It allows for housing batteries and the board inside a compact package.

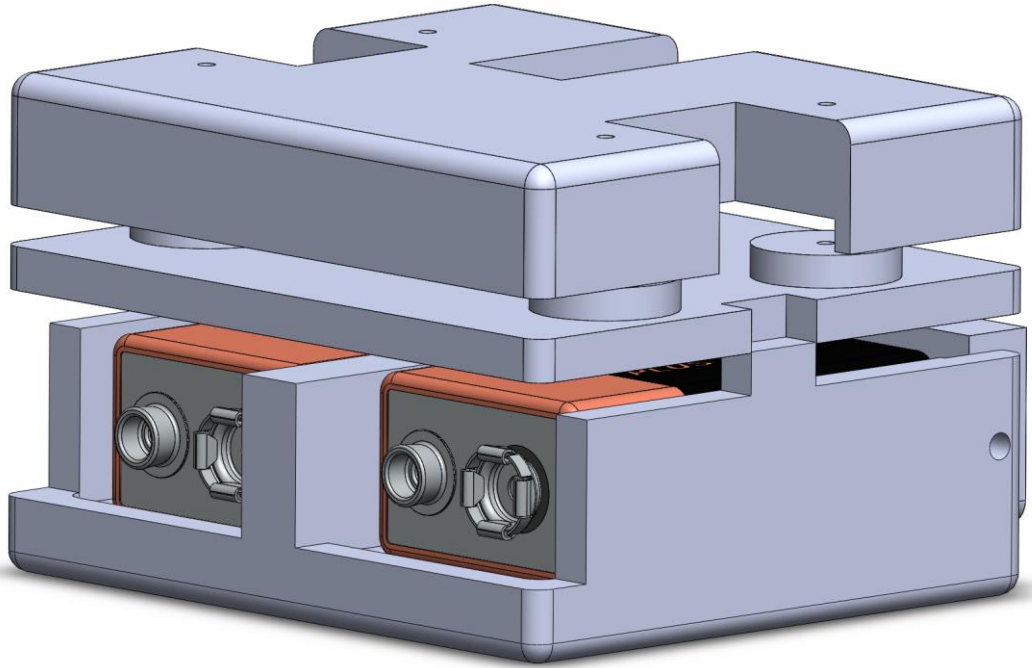


Figure 21: Enclosure design

Figure 21 shows the design of the enclosure. Enclosure has similar level of isolation between batteries that is used in the measurement board.

5 Verification

5.1 Nonlinearity Error Correction

As the AD8496 chip has fixed amplification, linearity error of the thermocouple voltage must be corrected to get more accurate results. Analog Devices make this correction quite simple, as they provide correction sheet in the applications notes of the AD8496 IC. This application note, called as AN-1087, provides correction table from -180°C to 1200°C , relevant part for this measurement is shown in Table 2.

Table 2: Relevant part of the nonlinearity error correction table reprinted from AN-1087 [22]

Thermocouple	AD8496	
Measurement Junction Temperature (°C)	Actual Output [mV]	Ideal Output [mV]
0	27	0
20	119	100
25	142	125
40	213	200
60	308	300
80	405	400
100	503	500
120	601	600
140	701	700
160	800	800
180	900	900
200	1001	1000

Error correction can be made in PicoScope software. While normal direct probes behave linearly, software allows user to make custom probes which can have nonlinear output. PicoScope uses interpolation to calculate values between known corrections, as the application note only cover values every 20°C.

While making this custom probe with error correction, output value can also be converted to Celsius degrees. Temperature output scaling on the AD8496 is 5mV/°C, thus voltage measurement can be divided by five for output to be shown directly as Celsius.

5.2 Board Verification

Correct operation of the board was verified with soldering iron, cold spray and oven. At first, thermocouple was installed into the board and measurement junction was heated with soldering iron. Heated measurement junction was then cooled with cold spray and temperature graph was checked using oscilloscope.

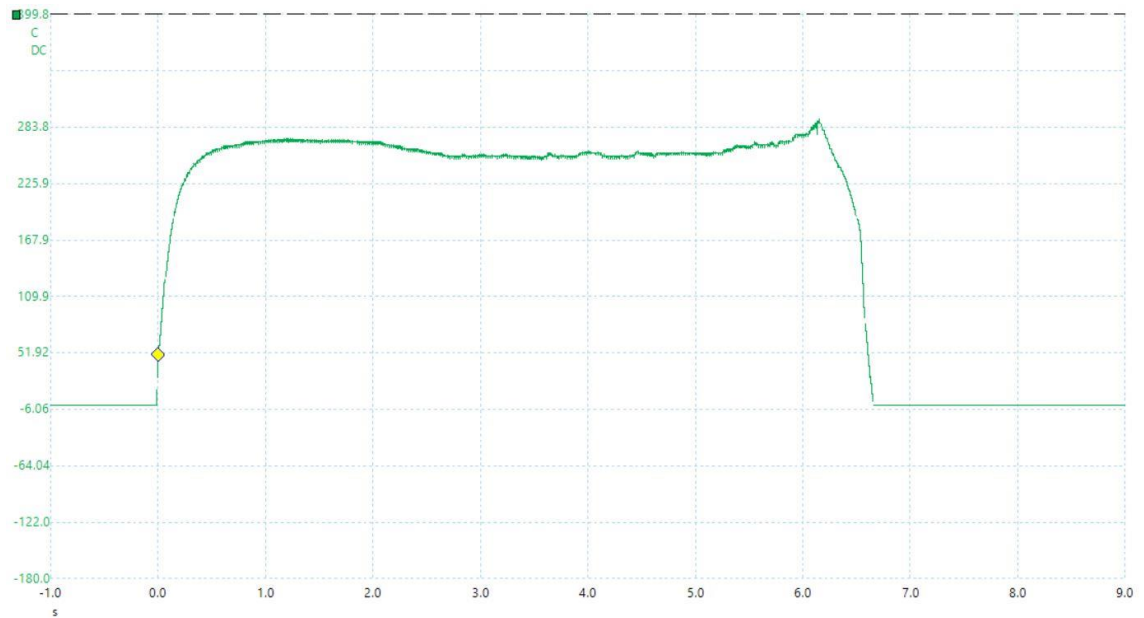


Figure 22: Temperature change response check

Figure 22 shows board behaving correctly when measurement junction was heated and cooled.

Accuracy testing was completed using electric oven. Fratelli manufactured G-Therm oven promises $\pm 0.3^{\circ}\text{C}$ temperature accuracy over the range of 0-260 $^{\circ}\text{C}$ [23]. When typical accuracy of an J-type thermocouple is 2.2 $^{\circ}\text{C}$ [24] and AD8496 IC promises max accuracy of 3 $^{\circ}\text{C}$ [20], this is enough to verify measurement board as a whole.

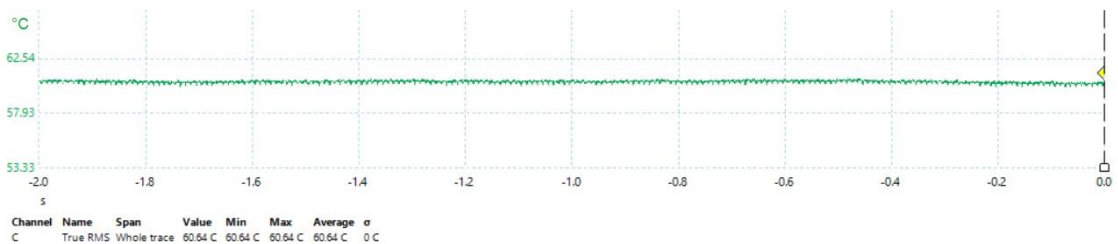


Figure 23: Measurement system accuracy testing

Thermocouple measurement junction was placed inside the oven and oven was set at 60 $^{\circ}\text{C}$. Figure 23 shows temperature reading of 60,64 $^{\circ}\text{C}$, which is a good accuracy for a thermocouple based measurement.

Last part of the verification was done later as part of the final measurements. It compares how the isolation amplifier affects the measurement results.

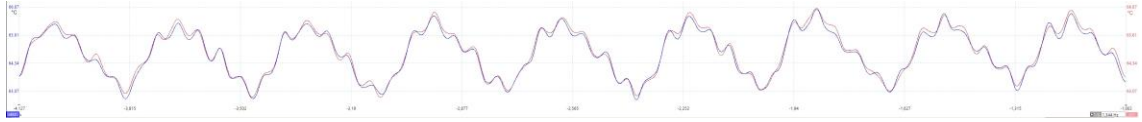


Figure 24: Comparison of non-isolated and isolated outputs

Figure 24 shows the effect of the isolation amplifier. Blue graph shows non-isolated output while red graph shows isolated output. Use of an isolating amplifier does not delay or affect the measurement in any way.

5.3 Initial Results

In the first measurements, switching noise highly affected the measurements results. Because of the switching noise, measurement signal needed to be highly filtered with a low pass filter to produce any kind of measurement. This unfortunately means that high frequency switching phenomena are lost.

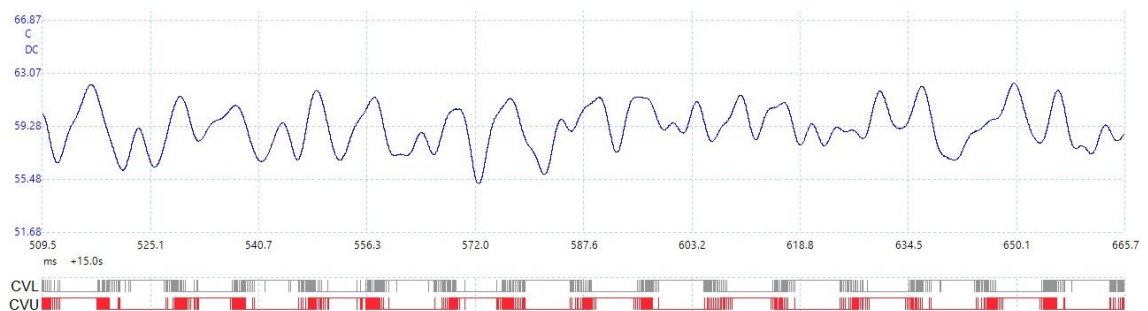


Figure 25: First measurements

Initial measurements can be seen on figure 25, the analog channel shows temperature reading and digital channel CVL shows lower side V-phase IGBT control signal. As can be seen from the results, temperature changes do not make any kind of sense. There does not seem to be any kind of correlation between IGBT control signals and the temperature reading.

5.4 Modifications

As from the start switching noise was known to be an issue, design included placements for optional filtering. At first, hardware RC filters were tested, but due to amount of work required to tune the filter, this was quickly stopped. PicoScope software includes a low pass filter, which is easily used and tuned within the software. This is a quick way to set required filtering frequency.

At first, even when using PicoScopes software filtering, results were not what was expected. First thoughts turned into Semikron provided MiniSKiiP modules and how thermocouple was installed inside of the module. Before X-raying the module to verify correct placement of the thermocouple, a few MiniSKiiPs with manually installed thermocouples were built. This method proved to be quite tricky, as the correct installation was quite hard and components inside the module were easily short circuited. Few correctly working prototypes was completed, but these MiniSKiiPs behaved similarly as those provided by Semikron, meaning most likely problems lied elsewhere.

Semikron provided MiniSKiiPs were also X-rayed afterwards to close out the possibility of improper installation of the thermocouple.

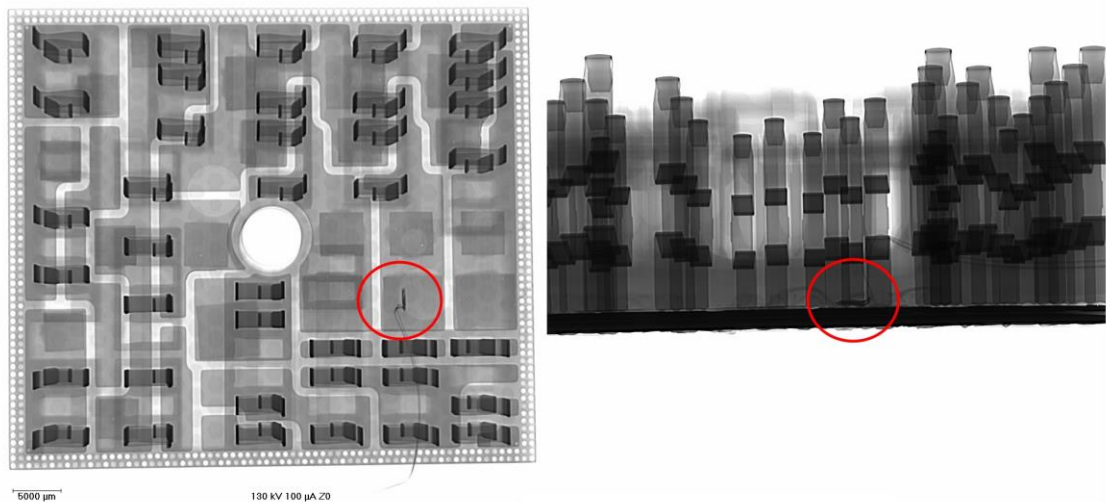


Figure 26: X-ray images of Semikron provided MiniSKiiP

As Figure 26 shows, thermocouple placement is correctly placed on the V-phase lower side IGBT. It is also notable how small the thermocouple measurement junction is, as its

thermal mass affects the temperature change response time. Most probably, as the actual thermal mass cannot be known just from the X-ray images, this installation would allow for large temperature changes in short time to be measured.

At this point, it was determined that it is not possible to measure temperature changes while IGBT switches using this measurement method. As the noise is magnitudes larger than the actual temperature change, it is too hard to filter and extract only the temperature change from the measurement.

First measurements were also done using 50Hz output frequency. Due to filtering requirements, higher output frequencies make it harder to distinguish actual IGBT junction temperature change. In the following measurements, load unit was set to keep load motor at standstill. ACS580 unit was then set to output maximum current using torque control. This resulted in quite stable 1.8Hz output frequency, making temperature change more noticeable.

5.5 End Results

While the system was designed to be fast enough to measure temperature changes when IGBT switches, one of other purposes was to compare temperature of the IGBT chip surface to temperature measured from heatsink. Normally IGBT chip temperature is measured from heatsink. This is done by drilling a hole to heatsink close to the chip and placing thermocouple into the hole.

In the next measurements, blue graph indicates IGBT junction temperature measurement and red graph shows temperature measured from heatsink.

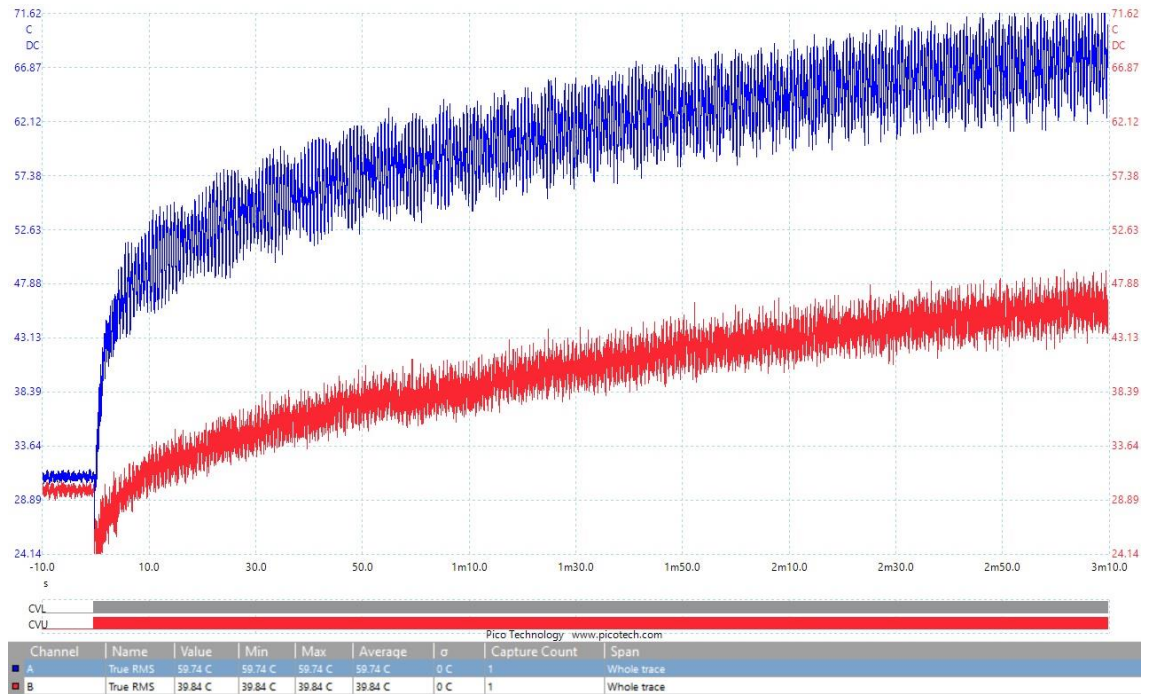


Figure 27: Comparison between junction and heatsink temperatures

Figure 27 shows IGBT and heatsink temperatures rising due to start of modulation. Modulation starts at the trigger point and IGBT temperature rises rapidly while stabilizing into lower rate of change towards the end. Heatsink temperature follows IGBT temperature, but due to having much higher thermal mass, not being actually connected to IGBT and being actively cooled by a fan, it does not ever reach the actual IGBT temperature. Also, as active cooling with a fan is started when modulation starts, heatsink temperature seems to dip a little bit at first.

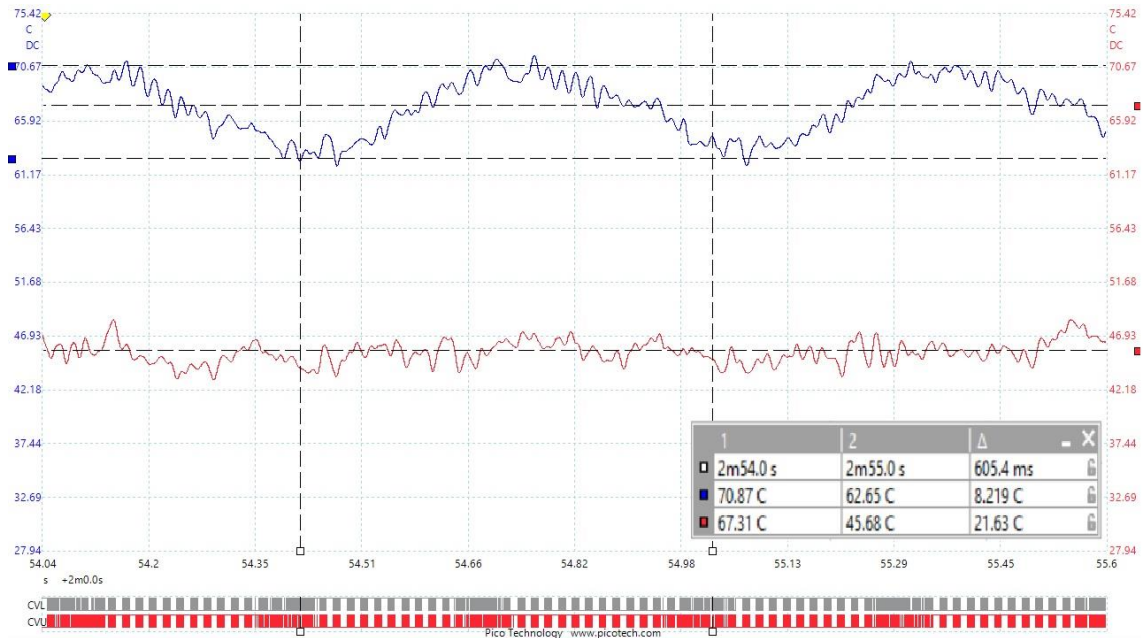


Figure 28: Lower side IGBT temperature change in one cycle

Predicted temperature change in IGBT follows the duty cycle of the control signal. Figure 28 shows this change, at about 8°C change per one cycle. Grey digital channel, CVL, shows the control signal of the measured IGBT. As the pulse width gets higher, IGBT junction temperature starts to increase. When pulse width starts to lower again, temperature starts to drop.

Figure 28 also shows the difference between temperatures on IGBT surface and heatsink. Previously, this was calculated to be around 20°C and if average temperature between these are compared, it shows a difference of around 21°C.

5.6 Future Considerations, Improvements and Measurements

As we did not get much information from Semikron about the thermocouple installation, more accurate information could be asked. For example, information on thermal response times, thermal mass, thermocouple placement or any validation measurements were not provided by Semikron. Based on simulations, even on ideal case, the measurement board would have a hard time measure temperature changes when IGBT

switches, but it is unknown if the thermal response time of the thermocouple is even fast enough to detect these.

One interesting test case for this system would be to compare actual IGBT junction temperature to values seen in software. Software does estimations for IGBT temperature measurement, so it would be interesting to see how close these estimations are to measured values.

Measurements could also be performed without the drive itself. Theoretically DC voltage could be connected straight into MiniSKiiP DC bus spring contacts, load to be connected to IGBT collector and external gate driver circuit used to drive the IGBT. This kind of setup would basically remove all the noise made by other IGBTs.

If higher frequency phenomena are to be measured while driving a motor, the biggest improvements on the system must come on filtering the noise. One obvious way to do that is to reduce noise before it even reaches the filter. Currently, thermocouple leads are installed as parallel cables which are quite ideal at picking radio-frequency interference when IGBT switches high current loads. Twisted pair thermocouple could already itself help drastically in noise reduction.

As far as filtering goes, digital programmable filtering could be used. Analog filters have four basic responses: low-pass, high-pass, band-pass and band-reject. Digital filtering allows completely custom filters to be programmed for multiple different frequencies to be filtered differently from each other. This solution would be better than what analog filters are able to do, but even using custom response filter, its highly possible that unwanted noise is just too large to completely filter out. DSP solution would also require very deep knowledge of the whole system, as it can be quite hard to predict what frequencies to filter out.

Completely different approaches could also be tested. Thermocouples will always be highly susceptible to noise, as the measured thermoelectric voltage is very small, thus even low amount of radio-frequency interference drastically changes measured temperature. Small NTC thermistors could be tried, as they still have quite high response time and are much more immune to noise than thermocouples.

6 Conclusions

IGBT surface temperature measurement proved to be as hard to measure as it was thought to be at the start of the project. Due to extra high amount of switching noise induced by high current switching in IGBT, temperature changes happening during switching could not be measured using this kind of approach.

Otherwise the design of the measurement board seems to be working properly. Board has good accuracy and isolation does not affect the temperature measurement at all. In some cases, such as running low output frequencies, temperature change on IGBT surface was detectable when heavily filtered.

These measurements also correspond to previous calculations regarding the difference between IGBT temperature measured from heatsink to the actual IGBT surface. This proves some parts of temperature estimations done by software to be correct.

References

- 1 ABB. Energy efficiency: Using drives to control motors can lead to big savings [online], 2018. URL: new.abb.com/drives/energy-efficiency. Accessed 8 November 2018.
- 2 Wikipedia. Cycloconverter [online], 2018. URL: en.wikipedia.org/wiki/Cycloconverter. Accessed 8 November 2018.
- 3 VFDs. What is VFD, How it works? - VFD working principle [online], 2018. URL: www.vfds.org/what-is-vfd-how-it-works-964803.html. Accessed 8 November 2018.
- 4 VFDs. What is a VFD? [online], 2018. URL: <https://www.vfds.com/blog/what-is-a-vfd>. Accessed 8 November 2018.
- 5 Electronics Tutorials. Insulated Gate Bipolar Transistor [online], 2014. URL: <https://www.electronics-tutorials.ws/power/insulated-gate-bipolar-transistor.html> Accessed 8 November 2018.
- 6 Power Electronics. Back-to-Basics: Power Semiconductors [online], 2012. URL: <https://www.powerelectronics.com/discrete-power-semis/igbts-frequently-asked-questions-faqs>. Accessed 8 November 2018.
- 7 EE Times. IGBT tutorial: Part 1 – Selection [online], 2007. URL: https://www.eetimes.com/document.asp?doc_id=1273173. Accessed 8 November 2018.
- 8 National Instruments. Sources of Loss [online], 2017. URL: <http://zone.ni.com/reference/en-XX/help/375482B-01/multisim/source-softloss>. Accessed 8 November 2018.
- 9 Wikipedia. Thermocouple [online], 2017. URL: <https://en.wikipedia.org/wiki/Thermocouple>. Accessed 8 November 2018.

- 10 University of Cambridge. Thermocouples: The Operating Principle [online], 2009. URL: www.msm.cam.ac.uk/utc/thermocouple/pages/ThermocouplesOperatingPrinciples.html. Accessed 8 November 2018.
- 11 Mosaic Industries. Thermocouple Types [online], 2018. URL: <http://www.mosaic-industries.com/embedded-systems/microcontroller-projects/temperature-measurement/thermocouple/types-wire-element>. Accessed 8 November 2018.
- 12 Analog Devices. Two Ways to Measure Temperature Using Thermocouples Feature Simplicity, Accuracy, and Flexibility [online], 2010. URL: www.analog.com/en/analog-dialogue/articles/measuring-temp-using-thermocouples.html. Accessed 8 November 2018.
- 13 Texas Instruments. Benefits and Reliability Advantages of Capacitive Isolated Amplifiers [online], 2016. URL: <https://training.ti.com/benefits-and-reliability-advantages-capacitive-isolated-amplifiers>. Accessed 8 November 2018.
- 14 Electronic Design. What's the Difference Between SAR and Delta-Sigma ADCs? [online], 2016. URL: <https://www.electronicdesign.com/adcs/what-s-difference-between-sar-and-delta-sigma-adcs>. Accessed 8 November 2018.
- 15 Texas Instruments. How delta-sigma ADCs work, Part 1 [online], 2011. URL: <http://www.ti.com/lit/an/slyt423a/slyt423a.pdf>. Accessed 8 November 2018.
- 16 ABB. Hardware manual ACS580-01 drives [online], revision E. URL: https://library.e.abb.com/public/13ace910b59d4897b90dfc7dda350eee/EN_ACS580-01_HW_E_A5_screen.pdf. Accessed 8 November 2018.

- 17 Semikron. Semikron MiniSKiiP Flyer [online], 2018. URL: <https://www.semikron.com/dl/service-support/downloads/download/semikron-flyer-miniskiiP-2018-05-08-enpdf.pdf>. Accessed 8 November 2018.
- 18 Semikron. SKiiP 24NAB12T4V1 [online], 2018. URL: <https://www.semikron.com/products/product-classes/igbt-modules/detail/skiiP-24nab12t4v1-25231420.html>. Accessed 19 November 2018.
- 19 Pico Technology. PicoScope® 3000 Series [online], 2018. URL: <https://www.picotech.com/oscilloscope/3000/usb3-oscilloscope-logic-analyzer>. Accessed 8 November 2018.
- 20 Analog Devices. AD849x Datasheet [online], revision D. URL: https://www.analog.com/media/en/technical-documentation/data-sheets/ad8494_8495_8496_8497.pdf. Accessed 8 November 2018.
- 21 Texas Instruments. AMC1311x Datasheet [online], 2018. URL: <http://www.ti.com/lit/ds/symlink/amc1311.pdf>. Accessed 8 November 2018.
- 22 Analog Devices. AN-1087 Application Note [online], 2010. URL: <https://www.analog.com/media/en/technical-documentation/application-notes/AN-1087.PDF>. Accessed 8 November 2018.
- 23 Fratelli Galli. Thermostatic Ovens G-Therm [online], 2018. URL: <https://www.fratelligalli.com/Galli-Ovens-GTherm-English.htm>. Accessed 8 November 2018.
- 24 Pico Technology. Improving the accuracy of temperature measurements [online], 2018. URL: <https://www.picotech.com/library/application-note/improving-the-accuracy-of-temperature-measurements>. Accessed 8 November 2018.

